important for analysis of the extremely crowded spectra of proteins since it provides a series of cross-checks on the spin system assignments. Multiple-quantum techniques are invaluable, by themselves and in conjunction with complementary methods, for unambiguously assigning the complex ^1H NMR spectra of proteins and other biological macromolecules.

Acknowledgments

We thank Prof. R. R. Ernst for providing a preprint of Ref. 38, Ms. L. Harvey for preparation of the manuscript, and the National Science Foundation (DMB-8517959 to M.R.) and the National Institutes of Health (NIH DK34909 and GM36643 to P.E.W.) for financial support.

[7] Detection of Insensitive Nuclei

By AD BAX, STEVEN W. SPARKS, and DENNIS A. TORCHIA

Introduction

Because of their larger chemical shift dispersions, ^{13}C and ^{15}N NMR spectra are often better resolved than the corresponding ^1H spectra. It was this particular feature that stimulated numerous heteronuclear NMR studies of proteins in the 1970s. The goal of these studies was to use measurements of ^{13}C and ^{15}N chemical shifts and relaxation rates to obtain information about molecular structure and dynamics. Unfortunately, the low sensitivity of ^{13}C and ^{15}N NMR necessitated the use of large sample quantities, and assignment of the ^{13}C and ^{15}N spectra was difficult, relying heavily on off-resonance decoupling techniques (provided that the attached protons were resolved and assigned).

The assignment problem has been greatly simplified by two-dimensional (2D) heteronuclear correlation spectra, in which the two coordinates of each resonance are the chemical shifts of a proton and of its directly attached heteronucleus. If the ^1H spectrum has been assigned, the heteronuclear correlation spectrum can be used to assign the corresponding ^{13}C and ^{15}N spectra. Alternatively, characteristic shifts to certain ^{13}C and ^{15}N nuclei are useful for assigning the ^1H NMR spectrum. The early 2D heteronuclear correlation techniques[1-4] were only partially successful for generating such correlation maps for proteins.[5-7] These methods relied on direct detection of the heteronucleus, the NMR amplitude of which was modulated by the frequency of its coupled proton(s). The major impediment of this approach was the low sensitivity of such methods, lower by at least a factor of three to five relative to a simple one-dimensional heteronuclear spectrum.

In more recently developed 2D correlation techniques the sensitive ^1H signal is detected, modulated by the frequency of its heteronuclear coupling partner, X. For historical reasons, this approach is often referred to as reverse correlation. Relative to a regular one-dimensional ^1H spectrum, the sensitivity of such a reverse-correlation map is decreased by the natural abundance of the heteronucleus (1.1% for ^{13}C and 0.37% for ^{15}N), but not by its magnetogyric ratio, γ_X. Maudsly *et al.*[2] pointed out the potential advantages of directly detecting the nucleus with the higher γ more than a decade ago. Subsequent work by Müller and Ernst,[8] Müller,[9] Bodenhausen and Ruben,[10] Bendall *et al.*,[11] Redfield,[12] and Bax *et al.*[13] paved the way for applying such techniques in a practical fashion.

This chapter describes a number of 2D reverse-correlation experiments that yield high-sensitivity heteronuclear correlation spectra. The optimal pulse sequence depends on the particular application and on the spectrometer used. For example, for correlation through long-range coupling or through one-bond coupling, different pulse schemes have to be used. Certain pulse schemes provide better suppression of artifacts but yield poorer line shapes.

This chapter is not a comprehensive review of heteronuclear correlation spectroscopy but rather a brief guide of what one may expect from such methods and how to record optimal spectra.

Sensitivity Gain from Reverse Correlation

There has been some confusion over what gain in sensitivity may be expected from the ^1H-detected heteronuclear correlation techniques.

[1] A. A. Maudsley and R. R. Ernst, *Chem. Phys. Lett.* **50**, 368 (1977).
[2] A. A. Maudsley, L. Müller, and R. R. Ernst, *J. Magn. Reson.* **28**, 463 (1977).
[3] G. Bodenhausen and R. Freeman, *J. Magn. Reson.* **28**, 471 (1977).
[4] A. Bax and G. A. Morris, *J. Magn. Reson.* **42**, 501 (1981).

METHODS IN ENZYMOLOGY, VOL. 176

[5] T. M. Chan and J. L. Markley, *J. Am. Chem. Soc.* **104**, 3010 (1982).
[6] J. L. Markley, W. M. Westler, T. M. Chan, C. T. Kojiro, and E. T. Ulrich, *Fed. Proc., Fed. Am. Soc. Exp. Biol.* **43**, 2648 (1984).
[7] W. M. Westler, G. Ortiz-Polo, and J. L. Markley, *J. Magn. Reson.* **58**, 384 (1984).
[8] L. Müller and R. R. Ernst, *Mol. Phys.* **38**, 963 (1979).
[9] L. Müller, *J. Am. Chem. Soc.* **101**, 4481 (1979).
[10] G. Bodenhausen and D. J. Ruben, *Chem. Phys. Lett.* **69**, 185 (1980).
[11] M. R. Bendall, D. T. Pegg, and D. M. Doddrell, *J. Magn. Reson.* **52**, 81 (1983).
[12] A. G. Redfield, *Chem. Phys. Lett.* **96**, 537 (1983).
[13] A. Bax, R. H. Griffey, and B. L. Hawkins, *J. Magn. Reson.* **55**, 301 (1983).

Numbers ranging from 10- to 1000-fold have been quoted in the literature. Here, the theoretical gain in sensitivity obtainable with the reverse-correlation method over the *X*-detected correlation technique will be briefly discussed.

The NMR sensitivity of a nucleus is proportional to $\gamma^{5/2}$.[14] Therefore, at a first glance, one might expect a gain in sensitivity of $(\gamma_H/\gamma_X)^{5/2}$ by directly detecting the proton instead of the *X* nucleus. However, in the *X*-detected experiment the sensitivity is improved by a factor γ_H/γ_X because of polarization transfer from ^{1}H to *X*. The expected gain in sensitivity is thus reduced to $(\gamma_H/\gamma_X)^{3/2}$. This number should be multiplied by the number of protons, *N*, directly attached to *X*; for the *X*-detected experiment, the amount of polarization transfer is nearly independent of *N*, whereas for reverse detection the detected signal is directly proportional to *N*. For ^{13}C–H correlation of methyl groups, the gain in sensitivity therefore equals $3 \times (4)^{3/2} = 24$, for methylenes it is 16, and for methine sites it is 8. For ^{15}N–H correlation of peptide amide resonances, the gain is about 30.

In the above discussion, the assumption has been made that ^{1}H and *X* nucleus line widths are identical. For $X = {}^{13}$C, ^{15}N, this assumption is generally incorrect for small molecules, where the ^{1}H resonance is often split by homonuclear *J* couplings. For macromolecules, however, the line width often is dominated by the heteronuclear dipolar coupling and will be quite similar for protons and for the *X* nuclei.

This entire sensitivity discussion has been restricted to the case where the quantity of sample is limited. If unlimited sample is available, the *X*-detection experiment can be performed in a large-diameter sample tube, improving its sensitivity significantly. Another practical consideration is that the so-called t_1 noise can be much worse in the reverse-correlation spectra. Finally, for successful reverse correlation it is essential to have some special hardware, including a reverse-detection probe.

Pulse Schemes for Reverse Correlation

A large variety of different heteronuclear reverse-correlation schemes has been proposed in the literature. No attempt will be made to review all these methods here, but the advantages and limitations of a small selection of such schemes will be discussed. The key to successful reverse-correlation experiments on natural abundance samples is that they should contain relatively few ^{1}H pulses. This facilitates suppression of the much stronger resonances from protons not coupled to the heteronucleus. The best schemes rely on the principle of heteronuclear multiple-quantum

[14] D. I. Hoult and R. E. Richards, *J. Magn. Reson.* **24**, 71 (1976).

coherence. Five different pulse schemes for correlation through one-bond couplings are shown in Fig. 1.

Zero- and Double-Quantum Correlation. Scheme a in Fig. 1 is the simplest, and it was first developed for correlating the imino protons in tRNA with their attached ^{15}N nuclei.[15] Scheme a (Fig. 1) can be used with or without decoupling of the heteronucleus and it can easily be adapted to studies in H_2O without presaturation by replacing the first ^{1}H pulse of Scheme a (Fig. 1) by one of the water-suppression schemes discussed by Hore.[16] This particular scheme, with the ^{1}H pulse replaced by a 2–1–4 Redfield pulse, was used by Glushka and Cowburn[17] for generating a high-quality ^{1}H–^{15}N shift correlation map of the amide resonances in basic pancreatic trypsin inhibitor (BPTI). Two disadvantages of Scheme a in Fig. 1 are that the acquired spectra cannot be phased to the absorption mode which necessitates the use of magnitude calculations in both dimensions of the 2D spectrum, decreasing resolution and sensitivity. Second, in Scheme a (Fig. 1) the detected ^{1}H signals are modulated by the zero- and double-quantum frequencies, corresponding to the sums and differences of the ^{1}H and *X* nucleus offsets from their respective carriers. Hence, analysis is less convenient because the 2D spectrum is not a conventional correlation map with ^{1}H chemical shifts along one axis and the *X* nucleus chemical shifts along the other axis. More serious is the fact that the ^{1}H signals are modulated by both zero- and double-quantum frequencies, i.e., the sensitivity of the experiment is decreased by $\sqrt{2}$ relative to the case where the ^{1}H signals are modulated by only a single frequency, the *X* nucleus chemical shift. Therefore, resolution and sensitivity of Scheme a (Fig. 1) are far from optimal, but its strong points are (1) the easy H_2O suppression and (2) a minimum amount of t_1 noise.

Constant-Time Heteronuclear Correlation. An interesting and underused variation of Scheme a (Fig. 1) has been developed by Müller *et al.*,[18] and is sketched in Scheme b (Fig. 1). Scheme b (Fig. 1) also employs a single ^{1}H excitation pulse, but it uses a constant duration of the evolution period through which an *X* nucleus 180° pulse is shifted in a stepwise fashion. Scheme b (Fig. 1) has several advantages over Scheme a (Fig. 1): Water suppression is even easier with Scheme b (Fig. 1) since the ^{1}H signal sampling is further removed from this pulse. Therefore, a relatively high receiver gain setting can be used, even for concentrated samples. In practice, Scheme b (Fig. 1) also gives the best suppression of signals not

[15] R. H. Griffey, C. D. Poulter, A. Bax, B. L. Hawkins, Z. Yamazumi, and S. Nishimura, *Proc. Natl. Acad. Sci. U.S.A.* **80**, 5895 (1983).
[16] P. J. Hore, this volume [13].
[17] J. Glushka and D. Cowburn, *J. Am. Chem. Soc.* **109**, 7879 (1987).
[18] L. Müller, R. A. Schiksnis, and S. J. Opella, *J. Magn. Reson.* **66**, 379 (1986).

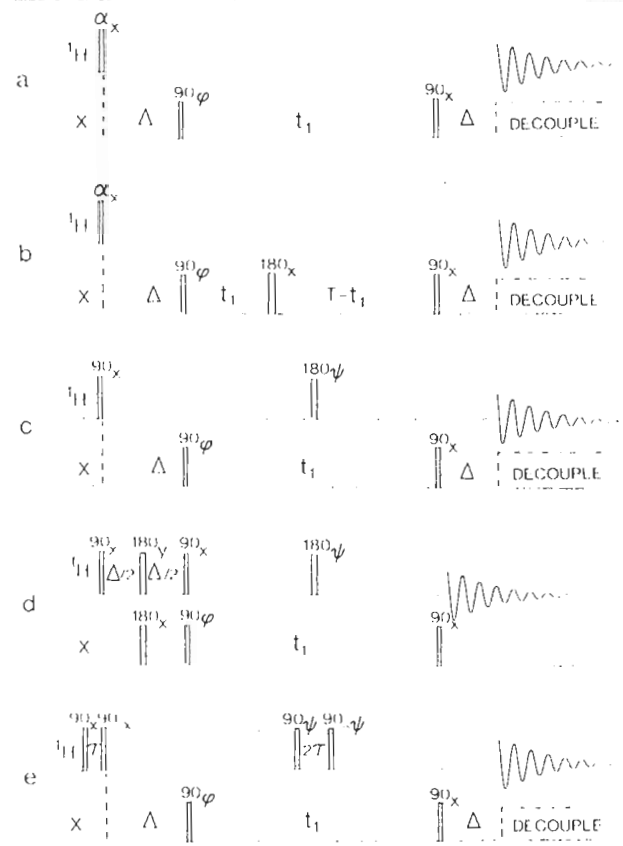

FIG. 1. Pulse schemes for heteronuclear correlation of protons with their directly attached X nuclei. All schemes employ ^{1}H detection. (a) Zero- and double-quantum correlation (absolute value). (b) Constant-time chemical shift correlation (absolute value). (c) HMQC chemical shift correlation (phase sensitive). (d) Flip-back chemical shift correlation (phase sensitive). (e) HMQC correlation in H_2O without presaturation (phase sensitive). For Schemes (a) and (b), the following phase cycling can be used (with TPPI incrementation of

coupled to the X nucleus. For a given time, T, between the 90° X pulses, the acquisition time in the t_1 dimension runs from $-T$ to $+T$, providing high resolution in the F_1 dimension. The acquired ^{1}H signals are modulated by the X nucleus chemical shift and not by the multiple-quantum frequencies (even while the "magnetization" exists as zero- and double-quantum coherence during the time T). Hence, the ^{1}H signals are modulated by only a single frequency, increasing sensitivity relative to Scheme a (Fig. 1). Finally, the spectrum conveniently displays X nucleus chemical shift frequencies along the F_1 axis. For best results, spectra should be acquired in the hypercomplex (or TPPI) fashion and the magnitude spectrum should be calculated in both dimensions. For digital filtering, a pseudo-echo filter is recommended in the t_1 dimension, with the signal at the edges of the t_1 time domain (at $t_1 = \pm T$) attenuated by about a factor of three relative to the center. In f_2, conservative filtering using, for example, a cosine bell, cosine-squared bell, or 60°-shifted sine (squared) bell is recommended. In all respects, this sequence is superior to Scheme a of Fig. 1 and it is surprising that this method has not found more application.

Heteronuclear Multiple-Quantum Correlation (HMQC). Scheme c (Fig. 1) is a simple modification of Scheme a (Fig. 1), where the zero- and double-quantum frequencies now are interchanged by the 180° ^{1}H pulse, applied at the center of the evolution period. This has the net effect of eliminating the ^{1}H chemical shift component from the multiple-quantum frequency. The final spectrum therefore has the appearance of a regular heteronuclear chemical shift correlation map, with ^{1}H chemical shifts along one axis and the X nucleus shift along the other axis. Neglecting the effect of small homonuclear couplings, this method permits the recording of pure absorption spectra, offering the highest possible resolution. Scheme c (Fig. 1) is often referred to as the HMQC (heteronuclear multiple-quantum correlation) or the "forbidden echo"[19] technique. A modified version[20] has been widely applied to the study of small molecules, and several applications of the HMQC scheme to natural abundance protein

[19] R. H. Griffey, A. G. Redfield, R. E. Loomis, and F. W. Dahlquist, *Biochemistry* **24**, 817 (1985).
[20] A. Bax and S. Subramanian, *J. Magn. Reson.* **67**, 565 (1986).

$\phi1$: ϕ_1 = x, −x; Acq = x, −x. For Schemes (c), (d), and (e): ϕ_1 = x, −x; ϕ_2 = x, x, −x, −x; ϕ_3 = x, −x, x, −x; Acq = x, −x, −x, x, −x, x, x, −x. To avoid poor cancellation of non-X coupled protons caused by imperfect steady state z magnetization (too short a delay time between scans), the phase of the final 90° X pulse and the receiver phase should be inverted after the eight-step cycle.[19]

studies have appeared.[21,22] Problems with the HMQC scheme are (1) suppression of signals from protons not coupled to X becomes more difficult by the addition of the 180° pulse, and (2) that recording the spectrum in H_2O solution is also more difficult [see discussion of Scheme e (Fig. 1) below]. The suppression of signals from protons not coupled to X improves with the square root of the number of scans and also is easier for relatively broad resonances. For proteins, the number of scans per t_1 value needed for sufficient signal to noise is usually quite large, on our Nicolet and Bruker spectrometers, so that suppression of signals not coupled to X does not present any practical problems in the study of macromolecules, provided that proper precautions are taken (e.g., no sample spinning).

As an example, Scheme e (Fig. 1) is applied to a sample of BPTI in D_2O, p²H 6.6, 7 mM, 70 mM NaCl, 35°. Figure 2 shows the C_α region of the HMQC spectrum, recorded at 600 MHz. The total measuring time was 11 hr. This spectrum was recorded with the same level for the ^{13}C pulses and the ^{13}C decoupling (3.3-kHz rf field), using WALTZ16 decoupling modulation.[23] Generating this 3.3-kHz rf field required about 3-W rf power, sufficiently high that sample heating and associated lock signal deterioration became significant. Therefore, the data acquisition time (t_2) (and the decoupling duration) was limited to 80 msec. WALTZ modulation with a 3.3-kHz rf field provides sufficiently good decoupling over an 8-kHz band width. A better choice for broad-band ^{13}C decoupling is to use the GARP modulation scheme,[24] covering nearly twice this band width with the same amount of rf power. However, to effectively excite this wider band width with the 90° pulses of the HMQC scheme, power switching between the ^{13}C pulses and the ^{13}C decoupling becomes essential, a feature not available on our spectrometer when the spectrum of Fig. 2 was recorded.

Most experimental work to date consistently avoids heteronuclear decoupling during ^1H data acquisition. However, it should be noted that heteronuclear decoupling doubles the signal-to-noise ratio (provided appropriate rf filtering is applied) and reduces signal overlap. Line shapes are otherwise unaffected.

Flip-Back Heteronuclear Correlation. If for instrumental limitations broad-band X nucleus decoupling is impossible, the original Scheme d (Fig. 1) proposed by Müller[9] may be preferable. In Scheme d (Fig. 1), the double $^1H/X$ 180° pulse eliminates the effects of ^1H offset during the first

[21] V. Sklenář and A. Bax, *J. Magn. Reson.* **71,** 379 (1987).
[22] A. Bax and L. Lerner, *Science* **232,** 960 (1986).
[23] A. J. Shaka, J. Keeler, T. Frenkiel, and R. Freeman, *J. Magn. Reson.* **52,** 335 (1983).
[24] A. J. Shaka, P. B. Barker, and R. Freeman, *J. Magn. Reson.* **64,** 547 (1985).

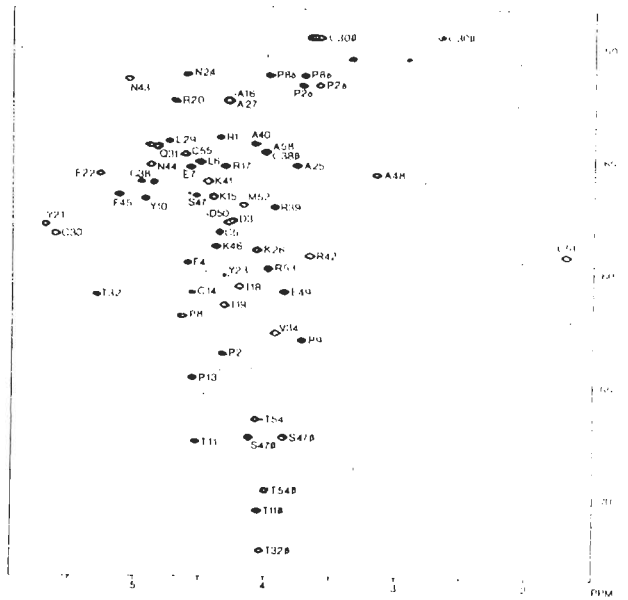

FIG. 2. C_α region of the ^1H–^{13}C shift correlation spectrum recorded at 600-MHz ^1H frequency, for a sample of 20 mg natural abundance BPTI in 0.5 ml D_2O. The measuring time was 11 hr. Assignments are taken from Wagner and Brunwhiler.[7] Acquisition times in the t_1 and t_2 dimensions were 50 and 70 msec, respectively. Sine bell digital filtering (45° shifted) and zero filling were used in both dimensions. TPPI type phase cycling was used.

delay, Δ, but leaves the heteronuclear coupling intact. The second ^1H 90° pulse flips the magnetization from protons not coupled to X to the $-z$ axis; magnetization from protons coupled to X is in antiphase along the $+x$ axis at this point in time and is converted into heteronuclear zero- and double-quantum coherence. The 180° ^1H pulse, applied at the midpoint of the evolution period, serves the same function as in Scheme c (Fig. 1), but has the additional effect of turning magnetization from protons not coupled to X back to the $+z$ axis. Spin diffusion then causes the rapid recovery of the longitudinal magnetization of the X-coupled spins. Two potential advantages of Scheme d (Fig. 1) are (1) that a somewhat faster

repetition rate can be used and (2) that (at least in principle) only signal from X-coupled protons reaches the receiver. This latter property decreases dynamic range problems and therefore can increase sensitivity of the experiment. In our experience, the flip back does *not* improve the cancellation of signals from protons not coupled to X. High-quality spectra using the flip-back scheme have been reported by Wagner and Bruewihler[25] (natural abundance ^{13}C of BPTI) and by Stockman *et al.*[26] (^{15}N-labeled flavodoxin).

Scheme d (Fig. 1) is less useful if X nucleus decoupling during data acquisition is required. ^1H chemical shifts are in phase at the end of the evolution period, whereas the decoupling should be started a time $1/(2J_{XH})$ later. In principle another set of double 180° pulses could be inserted between the final 90° X pulse and the start of data acquisition. In practice, if one wants to record decoupled spectra, Scheme e (Fig. 1) is probably preferable.

The heteronuclear coupled spectra, obtained with Scheme d (Fig. 1), are lower in signal-to-noise ratio by a factor of two relative to the decoupled spectra of Scheme e (Fig. 1) and show twice the number of resonances, i.e., an increased chance of overlap. In practice, the increased complexity of the spectrum may also have advantages. Several authors[17,25] state that the characteristic antiphase doublet pattern facilitates recognition of such heteronuclear correlations and may make it easier to distinguish them from artifacts and t_1 noise.

Very recently, Otting and Wuethrich[27] have proposed interesting modifications to Scheme d (Fig. 1) that would considerably alleviate the problem of suppressing signals from protons not coupled to X, with or without X nucleus decoupling. We have not yet had the opportunity to test the performance of these sequences, but results presented by these authors suggest that these schemes function quite well.

The 1–1 Echo Scheme. Correlating the backbone amide protons with their attached ^{15}N nuclei can be particularly valuable. It greatly improves the resolution in this region of the spectrum and the ^{15}N chemical shifts may contain structural information. Moreover, for cloned proteins, it is relatively easy to selectively ^{15}N-label certain types of amino acids, facilitating the assignment process and permitting the recording of edited NOESY and HOHAHA spectra.[19,28-31] As a first step, after ^{15}N incorporation in a protein, it is useful to record an ^1H–^{15}N correlation map. This usually gives much clearer results than a simple spin-echo difference spectrum[32] where partial overlap and low-level ^{15}N-labeling via transamination might be difficult to spot. To ensure that no amide resonances are lost due to presaturation, it is desirable to record these types of spectra with a sequence that avoids excitation of the water resonance, making presaturation unnecessary. A simple scheme for doing this is to replace the 90 and 180° ^1H pulses in Scheme e (Fig. 1) by jump-and-return 1–1[16] pulses (Scheme e, Fig. 1).[19] However, it should be noted that the 1–1 pulse at the center of the evolution period, which serves as a refocusing pulse, only works well over a relatively narrow frequency band. To obtain pure phase correlation spectra, phase cycling of this refocusing pulse unit therefore is essential.[33]

As an example, Fig. 3 shows the ^{15}N–^1H correlation spectrum obtained for the protein staphylococcal nuclease, complexed with pdTp and Ca^{2+}. Leucine, and to a lesser degree serine, were ^{15}N labeled. Spectra were recorded at 600 MHz, 35°, pH 7.4, 1.5 m*M*, 100 m*M* NaCl. Because of the ^{15}N labeling, high-sensitivity spectra can be obtained in a very short period of time. The spectrum of Fig. 3 was recorded in about 45 min, a minimum time dictated by the required phase cycling and the number of t_1 increments needed. The sample was also labeled with ^{13}C in the carbonyl position of lysine residues, giving rise to partially resolved doublet structures for Leu-7, Leu-25, Leu-137, and Ser-128, each of which are preceded by a lysine residue. At contour levels lower than shown, a large number of additional correlations become visible which probably correspond to glycine residues that carry an ^{15}N label derived from serine.

Heteronuclear Relay Experiments

One-bond heteronuclear correlations of isotopically labeled proteins are very sensitive experiments, comparable to the one-dimensional ^1H spectrum. Therefore, it is relatively straightforward to extend this type of experiment by combining it with NOESY, COSY, or HOHAHA.[29,27,31] Of the several dozen different pulse schemes available for these purposes, we discuss a single example: a combination of HOHAHA and heteronu-

[25] G. Wagner and D. Bruewihler, *Biochemistry* **25**, 5839 (1986).
[26] B. J. Stockman, W. M. Westler, E. S. Mooberry, and J. L. Markley, *Biochemistry* **27**, 136 (1988).
[27] G. Otting and K. Wuethrich, *J. Magn. Reson.* **76**, 569 (1988).
[28] A. Bax and M. Weiss, *J. Magn. Reson.* **71**, 571 (1987).
[29] R. H. Griffey and A. G. Redfield, *Q. Rev. Biophys.* **19**, 51 (1987).

[30] M. Rance, P. E. Wright, B. A. Messerle, and L. D. Field, *J. Am. Chem. Soc.* **109**, 1591 (1987).
[31] H. Senn, G. Otting, and K. Wuethrich, *J. Am. Chem. Soc.* **109**, 1090 (1987); S. W. Fesik, R. T. Gampe, and T. W. Rockway, *J. Magn. Reson.* **74**, 366 (1987).
[32] R. Freeman, T. H. Mareci, and G. A. Morris, *J. Magn. Reson.* **42**, 341 (1981).
[33] V. Sklenář and A. Bax, *J. Magn. Reson.* **74**, 469 (1987).

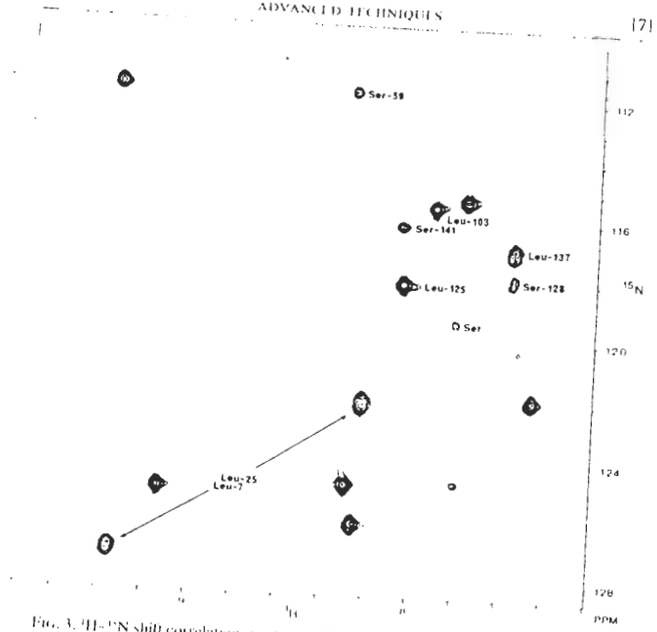

FIG. 3. ^{1}H–^{15}N shift correlation spectrum of labeled staphylococcal nuclease, recorded at 600 MHz. The spectrum was recorded with Scheme c of Fig. 1, using eight scans per t_1 value, preceded by two dummy scans. A 200 × 1024 data matrix was recorded, corresponding to acquisition times of 40 and 50 msec in the t_1 and t_2 dimension, respectively. The total measuring time was 45 min, but it should be noted that nearly one-half of this time was overhead for dummy scans and for writing the data to disk.

clear correlation. One of the possible pulse schemes for this purpose is sketched in Fig. 4. This sequence combines in a straightforward manner the pulse scheme (Scheme c in Fig. 1) with HOHAHA type mixing.[44,45] At the beginning of the MLEV17 mixing, the ^{1}H magnetization is aligned along the y axis and modulated in amplitude by the X spin chemical shift. The MLEV17 mixing scheme then redistributes the magnetization of the

[44] L. Braunschweiler and R. R. Ernst, *J. Magn. Reson.* **53**, 521 (1983).
[45] A. Bax and D. G. Davis, *J. Magn. Reson.* **65**, 355 (1985).

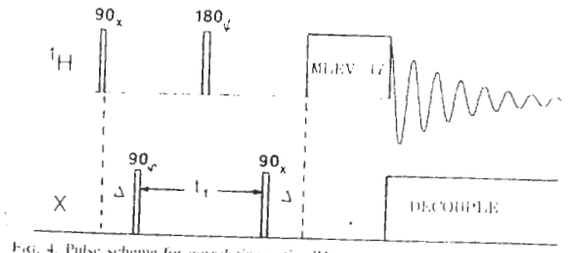

FIG. 4. Pulse scheme for correlating entire ^{1}H spin systems with a labeled X nucleus. Either the WALTZ or the MLEV scheme can be used for the homonuclear mixing (for details, see Bax [8], this volume). Phase cycling as in Fig. 1.

X-coupled proton over all its coupling partners. So, in the final 2D spectrum, all coupled protons will be modulated by the frequency of the X nucleus.

As an example, Fig. 5 shows the ^{13}C–^{1}H–^{1}H relay spectrum of [$^{13}C_\beta$] Ala-labeled staphylococcal nuclease, recorded at 500 MHz, 42 °, 1.5 mM in a 5-mm sample tube. The level of ^{13}C labeling was about 20%. The duration of the MLEV17 mixing period was set to 30 msec and no trim pulses[35] were used. At the beginning of the MLEV17 mixing, only magnetization from the methyl protons is modulated by the chemical shift of the ^{13}C. The MLEV17 transfers magnetization from the methyl protons to the C_α proton, resulting in correlations between C_αH and $^{13}C_\beta$. This spectrum provides significant simplification compared to a simple direct 2D HOHAHA spectrum (compared with Fig. 5, Bax [8], this volume). Future developments are expected where such experiments are performed in a three-dimensional fashion,[46] permitting the use of much more extensive labeling without introducing spectral overlap.

Correlation via Small Couplings

There is, of course, no fundamental difference between correlation via direct or via long-range couplings. However, there are large practical differences in how to optimize the experiment and what pulse sequence to choose. Problems in correlating chemical shifts of protons and heteronuclei via long-range couplings are that (1) the size of the couplings show large variations, (2) the heteronuclear couplings are typically of the same

[46] H. Oschkinat, C. Griesinger, P. J. Kraulis, O. W. Sorensen, R. R. Ernst, A. M. Gronenborn, and G. M. Clore, *Nature (London)* **332**, 374 (1988).

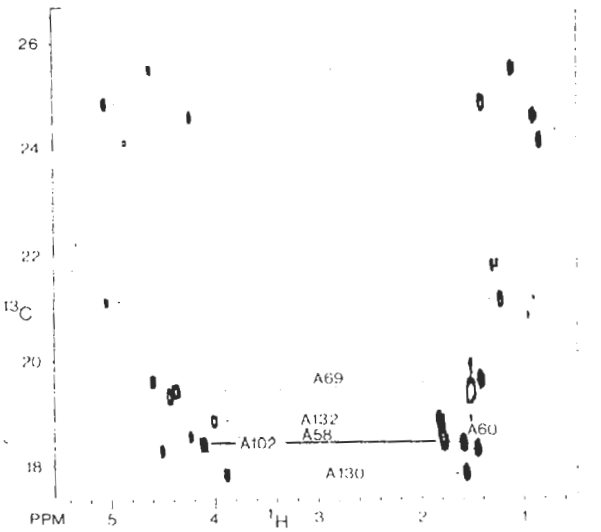

FIG. 5. Example of an HOHAHA ^{13}C relay spectrum recorded with the scheme of Fig. 4, using an MLEV-17 mixing scheme with a total duration of 30 msec. The sample of staphylococcal nuclease was about 20% [$^{13}C_\alpha$]Ala. For every methyl group, the corresponding C$^\alpha$H is clearly observed. The spectrum was recorded at 500 MHz, 42°, using a total measuring time of 12 hr. Resonances not connected by horizontal bars originate from natural abundance signals.

order of magnitude as the homonuclear ^1H–^1H couplings, and (3) in macromolecules the heteronuclear long-range couplings are often smaller than the natural line widths of the proton resonances. As a consequence, in macromolecules the sensitivity of long-range correlation experiments is reduced dramatically relative to the correlation through one-bond couplings, described above. For the study of proteins at low concentrations, isotopic labeling is therefore always essential.

Our discussion is limited to one sequence that yields long-range correlation spectra, although it should be realized that this particular sequence is not necessarily the best for all applications. Its pulse scheme is

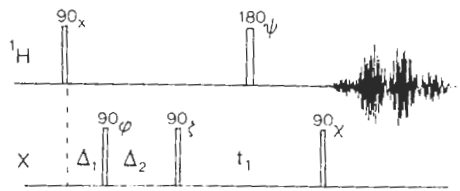

FIG. 6. Scheme for ^1H-detected heteronuclear multiple-bond correlation (HMBC) via multiple-quantum coherence. The delay, Δ_1, and the first 90° X pulse serve to suppress direct X–H correlations (J filter[37]). For correlation to X nuclei that do not have directly attached protons, Δ_1 should be set to zero and the 90° pulse may be omitted. The phase cycling (with TPPI incrementation of ζ) is ϕ = x, -x, y, -y; χ = x, -x; φ = x, -x; Acq = x, -x, -x, x, -x, x, x, -x. The phase cycling of χ serves to eliminate effects of changes in the steady-state z magnetization,[38] introduced by the phase cycling of ϕ. After 16 steps, the phase ϕ may be inverted (J filter) without changing the receiver phase.

sketched in Fig. 6,[37,38] and inspection shows that this scheme is nothing but a slightly modified version of Scheme c (Fig. 1). This sequence, first applied to long-range ^1H–^{13}C correlation in coenzyme B_{12},[39] is known under the name HMBC, for heteronuclear multiple-bond correlation. The first (optional) 90° X pulse serves as a 1D J filter,[37] to eliminate one-bond correlations from the 2D spectrum. The second 90° pulse, applied after another delay Δ_2, creates the multiple-bond multiple-quantum coherence. The 180° pulse removes the ^1H chemical shift contribution and the final 90° X pulse converts the multiple-quantum coherence back into antiphase ^1H magnetization. No X decoupling is applied during data acquisition.

Because of homonuclear ^1H–^1H couplings it is not possible to obtain absorption mode spectra in the F_2 dimension of the 2D spectrum. However, in the F_1 dimension the data are simply modulated in amplitude by the X chemical shift and an absorption mode representation in this dimension can be obtained.[40] Because the data are in antiphase at the beginning of the detection period, t_2, the time domain signal in the t_2 dimension starts at zero; it is a sine function that is rapidly damped by the short T_2 of the protons. For sensitivity purposes it is best to apply a matched filter to

[37] H. Kogler, O. W. Sorensen, G. Bodenhausen, and R. R. Ernst, *J. Magn. Reson.* **55**, 157 (1983).
[38] J. Cavanagh and J. Keeler, *J. Magn. Reson.* **77**, 612 (1988).
[39] A. Bax and M. F. Summers, *J. Am. Chem. Soc.* **108**, 2093 (1986).
[40] A. Bax and D. Marion, *J. Magn. Reson.* **78**, 186 (1988).

these data, i.e., in the t_2 dimension a nonshifted sine bell is a suitable function if the data acquisition time in the t_2 dimension is set to about $2–3 \times T_2$.

As an example, the scheme of Fig. 6 is applied to a sample of staphylococcal nuclease complexed with pdTp and calcium. Fourteen milligrams of the complex (18 kDa) was dissolved in 0.5 ml D_2O and spectra were recorded at 600 MHz, 35°, p²H 7.4. Figure 7 shows the long-range $^1H–^{13}C$ correlation spectrum for a sample where threonine residues are labeled

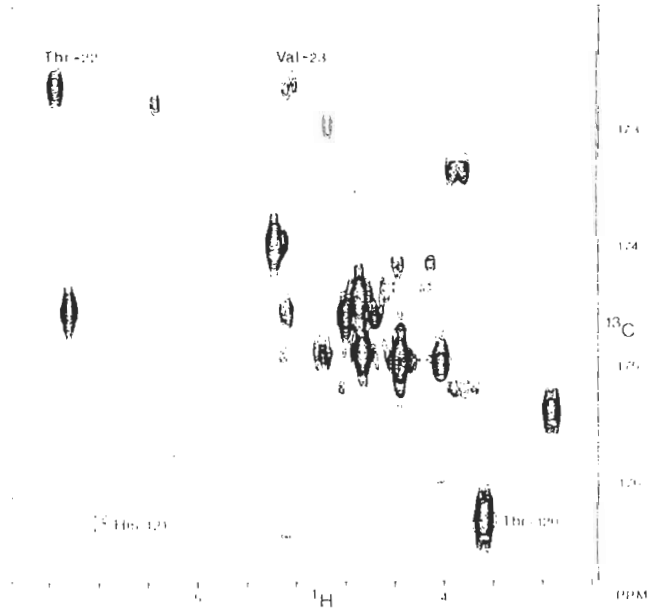

FIG. 7. Six hundred megahertz $^1H–^{13}C$ correlation of staphylococcal nuclease, recorded with the scheme of Fig. 6. The protein was labeled in the carbonyl position of the 11 Thr residues. Experimental details: Acquisition times in the t_1 and t_2 dimensions, 40 and 102 msec; sine bell filter in t_2, 60° shifted sine bell in t_1, $\Delta_1 = 0$, $\Delta_2 = 33$ msec; total measuring time 14 hr; absorption mode in F_1, absolute value in F_2. Because more than 11 ^{13}C chemical shifts are observed in this spectrum, it is suspected that some of the low-intensity correlations originate from natural abundance or low-level ^{13}C-labeled amino acids other than Thr.

with ^{13}C in the carbonyl position. A large number of cross-peaks can be seen, corresponding to the 11 different threonine residues present in the protein. The intensities of the correlations vary dramatically, the difference between the highest and lowest contour level in Fig. 7 is a factor of 48. These intensity differences reflect the different sizes of the long-range couplings and the differences in line width of the $C_\alpha H$ resonances. In practice, only two- and three-bond couplings can be sufficiently large to yield observable correlations. The size of $^2J_{CH}$ depends strongly on conformation and up to four correlations (three for threonine) in principle can be observed for a single carbonyl resonance (two C_α protons and up to two C_β protons for most amino acids). However, in practice many of these possible correlations have too low an intensity to be observable in proteins of the size of staphylococcal nuclease. This is unfortunate because otherwise this type of correlation would be extremely valuable for obtaining sequential assignments. Two examples of such sequential assignment are labeled in Fig. 7; both the C_α protons of Thr-22 and Val-23 show a correlation to the carbonyl of Thr-22 and similarly, His-121 $C_\alpha H$ and Thr-120 $C_\alpha H$ show connectivity to the carbonyl of Thr-120. Of course, it would be of major interest to also correlate the NH resonances with the labeled carbonyls. However, for the staphylococcal nuclease complex, the T_2 values of the NH resonances were too short (11–13 msec) to permit this type of correlation to be observed.

The example shown here is only one of the many different applications of the ^1H-detected methodology. Other very interesting applications of long-range heteronuclear correlation in proteins concern the detection of metal nuclei (Cd,[41,42] Hg,[43] Pt) and phosphorus.[44] In cases where the T_1 of the heteronucleus is shorter than the T_1 of the protons but its T_2 is not shorter than the T_2 of the protons, a different sort of approach, not based on multiple-quantum coherence may be favorable.[45]

Discussion

The heteronuclear two-dimensional experiments discussed in this chapter show particular promise for alleviating assignment problems in proteins. Although the one-bond correlation techniques, at least in princi-

[41] M. H. Frey, G. Wagner, M. Vasák, O. W. Sørensen, D. Neuhaus, E. Wörgötter, J. H. Kägi, R. R. Ernst, and K. Wüthrich, *J. Am. Chem. Soc.* **107**, 6842 (1985).
[42] J. D. Otvos, H. R. Engeseth, and S. Wehrli, *J. Magn. Reson.* **61**, 579 (1985); D. Live, I. M. Armitage, D. C. Dalgarno, and D. Cowburn, *J. Am. Chem. Soc.* **107**, 1775 (1985).
[43] D. A. Vidusek, M. F. Roberts, and G. Bodenhausen, *J. Am. Chem. Soc.* **104**, 5452 (1982).
[44] D. H. Live and D. F. Edmonson, *J. Am. Chem. Soc.* **110**, 4468 (1988).
[45] V. Sklenář, H. Miyashiro, G. Zon, H. T. Miles, and A. Bax, *FEBS Lett.* **208**, 94 (1986).

ple, could be applied to natural abundance samples of small proteins, the most promising area of application is for ^{13}C- and ^{15}N-labeled proteins that are too large for straightforward analysis. These techniques then can be combined with NOESY and HOHAHA methods to obtain spectra of reduced complexity. Alternatively, three-dimensional NMR techniques that are based on combining HOHAHA or NOESY with heteronuclear correlation are expected to become of major practical relevance for NMR analysis of proteins. Although the use of one-bond heteronuclear correlations is largely limited to solving assignment problems, the multiple-bond correlations also carry structural information since the intensities of the correlations reflect the size of the heteronuclear J couplings.

For the methods discussed in this chapter it is essential to have access to a so-called "inverse probehead," with the ^1H observe coil close to the sample (for the highest possible sensitivity) and the decoupler coil on the outside. Despite the fact that the regular so-called "dual probe" may function quite well for regular proton observation, its sensitivity for the inverse correlation experiments is dramatically lower. In our experience the inverse probe shows the same sensitivity (within 10%) and line shape as the regular ^1H-dedicated probehead and, as a result, in our laboratory we typically leave the inverse probehead in the magnet for months at a time, saving instrument time and reducing the possibility of damage. All experiments are relatively "risk free," provided that the system is protected from an overdose of X nucleus decoupling power.

Currently, almost all spectrometers (even new ones) are designed to directly detect heteronuclei, and at best, inverse detection options have been added as an afterthought. We expect this situation will change during the next few years, and application of the heteronuclear correlation techniques may then become as straightforward as the present recording of COSY and NOESY spectra.

[7] L. Lerner and A. Bax, *J. Magn. Reson.* **69**, 375 (1986).